

Precipitation Processes in Al-4Cu-(Mg, Cd) (wt. %) Alloys

Bondan T. Sofyan¹, Ian J. Polmear¹ and Simon P. Ringer²

¹School of Physics and Materials Engineering, P.O. Box 69 M,
Monash University, VIC 3800, Australia

²Australian Key Centre for Microscopy & Microanalysis,
The University of Sydney, NSW 2006, Australia

Keywords: Cd, Cd-Mg, cluster, θ' , σ , Al-Cu-Mg alloys, 3DAP, TEM

Abstract. The precipitation processes during elevated temperature ageing of Al-4Cu-(Mg, Cd) (wt. %) alloys have been studied using transmission electron microscopy and three dimensional atom probe (3DAP). Enhanced precipitation of θ' (Al_2Cu) was confirmed in Cd-containing alloys. Additions of Cd into the Al-Cu-Mg alloys also stimulated the precipitation of the σ phase ($\text{Al}_5\text{Cu}_6\text{Mg}_2$). In the ternary Al-Cu-Cd alloy, elemental Cd particles were detected in a uniform dispersion throughout the matrix and were attached to θ' , while in the Al-Cu-Mg-Cd alloy, co-clustering of Cd-Mg was observed at early stages of ageing. This result suggests that the enhanced precipitation and associated hardening in the quaternary Al-Cu-Mg-Cd alloy is initiated by the Cd-Mg co-clusters, through what is called as cluster-assisted nucleation. The nucleation mechanism in the ternary Al-Cu-Cd alloy is almost certainly the same, although the chemistry of the initiating cluster which assists nucleation is different, which is thought to be Cd clusters.

Introduction

It is well known that microalloying additions to Al alloys can influence the precipitation process and this has practical importance in their applications as structural alloys. For example, Al-Cu alloys microalloyed with Cd, Sn and In are known to have a finer dispersion of θ' and exhibit an increased hardening response [1-3]. Although various mechanisms have been proposed to account for this effect, one-dimensional atom probe (1DAP) experiments on an Al-1.7Cu-0.01Sn (at. %) alloy have shown that θ' nucleation is preceded by clustering of Sn atoms and the precipitation of β -Sn. The fine and uniform dispersion of θ' which follows forms so that the β -Sn particles are associated with the incoherent rim of the precipitates [4]. Furthermore, Kanno *et al.* [5] have observed In particles in Al-Cu-In alloys and Nie *et al.* [6] have recently discussed the enhanced precipitation of θ' in Al-Cu-Sn/In alloys in terms of cluster-assisted nucleation.

Minor additions of Mg to Al-Cu alloys are known to promote $\{120\}_\alpha$ types of precipitates, such as S (Al_2CuMg) [7], and using 1DAP, it was shown recently that Mg-Cu co-clusters predominate during the early stages of ageing in ternary Al-Cu-Mg alloys [8]. Combined additions of Cd and Mg are known to promote a fine dispersion of θ' which enhances hardening in Al-Cu-Mg-Cd alloys [9]. In this case, it seems that Cd atoms remain available to assist nucleation of θ' since there are no known stable compounds formed between Cd and Mg [10],

The present work examines the effects, in more detail, of Cd and Mg, both individually and in combination, on precipitation processes in Al-4Cu-(Mg, Cd) (wt. %) alloys aged at 200 °C, by using transmission electron microscopy and the newly installed three-dimensional atom probe (3DAP) at Monash University.

Experimental

Three alloys were used in this study and their nominal compositions (in wt. %) are: (i) Al-4Cu-0.3Mg; (ii) Al-4Cu-0.3Cd and (iii) Al-4Cu-0.3Mg-0.5Cd. Samples of each were cut into 10 x 10 mm blocks for hardness testing, 0.3 x 0.3 x 10 mm needles for 3DAP, or were rolled to ~ 200 μm for TEM. After solution treatment at 525 $^{\circ}\text{C}$ for 1 h and cold water quenching, ageing was conducted at 200 $^{\circ}\text{C}$. Hardening response was monitored by Vickers hardness measurements using a 5-kg load. The evolution of microstructure was followed by means of a Philips CM20 analytical scanning transmission electron microscope (ASTEM) operating at 200 kV. Samples for ASTEM were prepared in a twin jet polisher using a solution of 1:2 vol. % nitric acid:methanol at -25 $^{\circ}\text{C}$. Samples for 3DAP were prepared by electropolishing the needles, initially in nitric acid containing few drops of water, and then in a solution of 3 % perchloric acid in 2-butoxyethanol to sharpen the tips. Three dimensional atom probe analysis was carried out at 20K with a pulse fraction of 25 % in an ultra high vacuum of 1.3×10^{-11} mbar.

Results

Age Hardening Response. The age hardening curves of the alloys following ageing at 200 $^{\circ}\text{C}$ are presented in Fig. 1. Each shows single stage hardening that is a characteristic of many Al-Cu based alloys. An incubation period of ~15 min was observed in all alloys, followed by an increase to peak hardness. The curves confirm previous results that the addition of Cd increases the peak hardness and reduces the time to reach peak hardness [1]. It may be noted that combined additions of Cd and Mg result in a higher peak hardness than if the alloy contain only one of these elements.

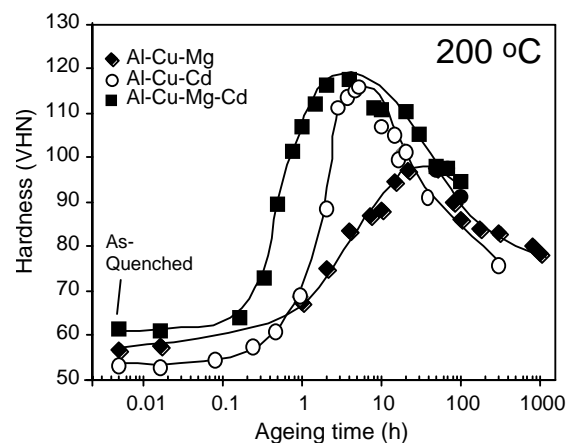


Fig.1 Age hardening curves following ageing at 200 $^{\circ}\text{C}$.

Precipitation Processes. The as-quenched microstructures of the three alloys were relatively free from defects and no dislocation loops were observed, which is attributed to the high binding energy between Cd, Mg atoms and vacancies.

Bright field (BF) TEM images of the peak hardness microstructure for each alloy during ageing at 200 $^{\circ}\text{C}$ were recorded close to the $\langle 001 \rangle_{\alpha}$ zone axis and examples are provided in Fig. 2. The Al-Cu-Mg alloy microstructure is dominated by coarse plates, Fig.2 (a), and the corresponding SAED pattern shows reflections at $\{110\}_{\alpha}$ positions and sharp streaks emerging from those positions parallel to the $\langle 001 \rangle_{\alpha}$ direction, which are consistent with θ' phase. The S and σ precipitates were occasionally observed in this alloy.

Fig. 2 (b) is the peak hardness microstructure of the Al-Cu-Cd alloy which consists of a denser and more uniform distribution of θ' precipitates, together with a finer dispersion of much smaller, spherical particles. Some of these nanoscale particles formed independently in the α matrix and some of them are attached to the θ' phase. This microstructure is in excellent agreement with that reported previously [5]. The corresponding SAED pattern again shows reflections and streaks consistent with the diffraction effects of the θ' phase.

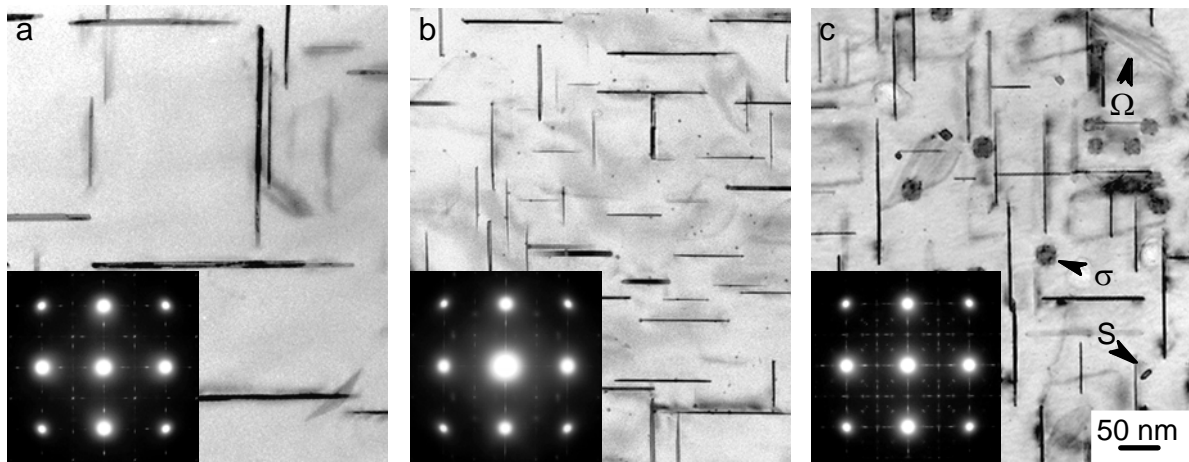


Fig.2 Peak hardness microstructures and corresponding SAED patterns of (a) Al-Cu-Mg; (b) Al-Cu-Cd and (c) Al-Cu-Mg-Cd alloys. Electron beam was parallel to the $\langle 001 \rangle_{\alpha}$ direction.

The peak hardness microstructure of the quaternary Al-Cu-Mg-Cd alloy consists mainly of the θ' and a second phase that was identified as σ ($\text{Al}_5\text{Cu}_6\text{Mg}_2$, $Pm\bar{3}$, $a = 0.831$ nm). [11] (Fig. 2(c)). In addition, occasional Ω precipitates (Al_2Cu , $Fm\bar{m}m$, $a=0.496$ nm, $b=0.859$ nm and $c=0.848$ nm) [12] on $\{111\}_{\alpha}$ planes were also observed and these are inclined to the beam direction in this figure. Some S phase (Al_2CuMg , $Cmcm$, $a=0.404$ nm, $b=0.925$ nm and $c=0.718$ nm) precipitates were also detected, as identified by the characteristic $\{210\}_{\alpha}$ trace. Careful inspection of the BF TEM images revealed that there were small particles attached to both the θ' and σ phases. These particles were usually located at the edges or corners of the precipitates (see also Fig. 3(a)). Similar to the Al-Cu-Cd alloy, a dispersion of small spherical particles was also detected uniformly throughout the matrix.

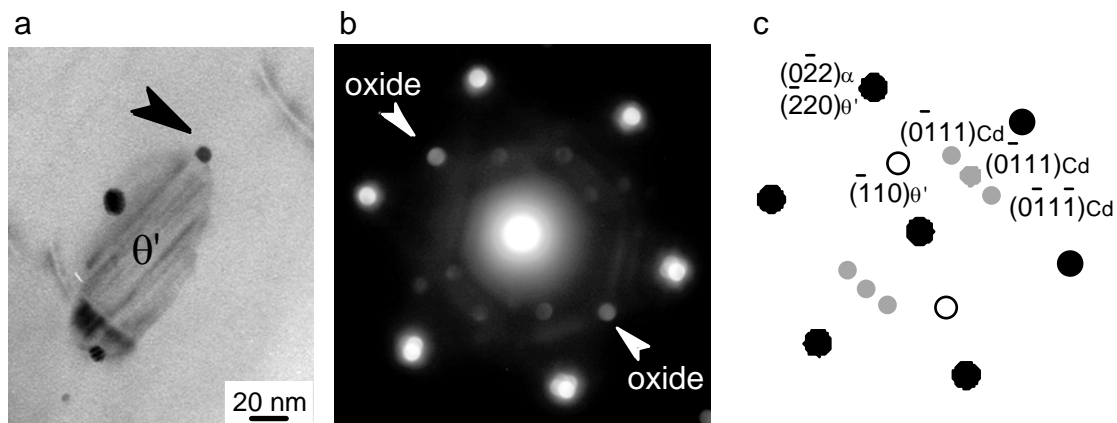


Fig.3 (a) $\langle 111 \rangle_{\alpha}$ BF TEM micrograph of the Al-Cu-Cd alloy aged at 200 °C for 200 h, showing a θ' with small precipitates attached to it. (b) MBED pattern of the small precipitate arrowed in (a). (c) Indexed pattern based on θ' and Cd structures.

Special attention has been paid to the small particles observed in the matrix and those attached to larger precipitates in both the Al-Cu-Cd and Al-Cu-Mg-Cd alloys aged at 200 °C. Earlier, it was shown that, in the latter alloy, the small particles in the matrix are elemental Cd, whereas those attached to the θ' and σ phases contain both Cd and Mg [13]. Fig. 3 (a) shows a large precipitate of θ' in an overaged Al-Cu-Cd alloy which appears to be encircled by several surface dislocations. Small spherical particles ~ 4 nm in size are attached to the edges of θ' precipitate and a microbeam electron diffraction (MBED) pattern from the region of one of these particles (arrowed) is shown in Fig. 3 (b). It is clear that this pattern may be indexed as both θ' and elemental Cd (hexagonal, mmc , $a=0.298$ nm, $c=0.562$ nm) as simulated in Fig. 3(c). The Cd precipitates were observed to bear a simple orientation relationship with

the matrix: $\{111\}_\alpha // \{0001\}_{\text{Cd}}$; $\langle 110 \rangle_\alpha // \langle 11\bar{2}0 \rangle_{\text{Cd}}$ [14]. The small precipitates in the matrix were also confirmed to be elemental Cd. These results verify that the small precipitates either distributed throughout the matrix or attached to θ' in the Al-Cu-Cd alloy are elemental Cd particles, as suggested by Sankaran and Laird [15].

Although the microstructure of the peak hardness and overaged conditions successfully confirm that the addition of Cd stimulates the θ' precipitation in both the Al-Cu-Cd and Al-Cu-Mg-Cd alloys, and are in good agreement with previous observations [1-5, 9, 15], the early stages of precipitation remain unclear and need to be resolved. Therefore, 3DAP experiments were conducted on the underaged Al-Cu-Mg-Cd samples.

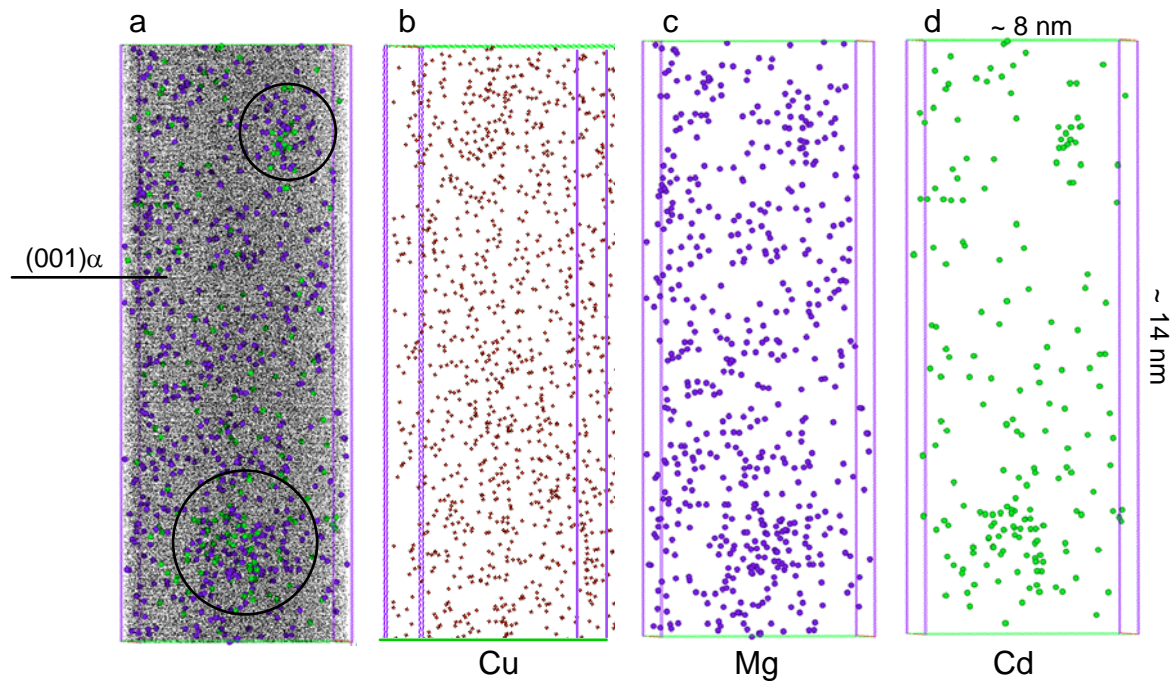


Fig.4 (a) Elemental mapping of Al-Cu-Mg-Cd alloy aged at 200 °C for 15 min, showing the presence of two clusters. Separate maps of (b) Cu; (c) Mg and (d) Cd atoms.

Statistical analysis of the 3DAP results on the Al-Cu-Mg-Cd alloy aged at 200 °C for 30 s showed that there is an early tendency of the co-segregation of Cd and Mg (results not shown here). Then after 15 min, solute clusters were observed to be dispersed uniformly throughout the sample with spacing of $\sim 15 \text{ nm}$. An example of atomic maps showing two such solute clusters is provided in Fig. 4 (a), where the layers of $(001)_\alpha$ planes are clearly resolved. The maps showing the positions of individual species of solute atoms are presented separately in Fig. 4(b) – (c). It is clear that Mg and Cd atoms co-segregate in the cluster. The shape of the clusters was roughly spherical and they contain a large number of Al atoms together with Cd, Mg and Cu atoms. The average Cd:Mg:Cu ratio of the clusters was found to be $\sim 1:1:1$ with the numbers of solute atoms incorporated in each cluster varying from 70 – 100.

To confirm the likelihood of the initial Cd-Mg co-segregation, 4 x 4 contingency tables were constructed for Cd-Mg, Cu-Mg and Cu-Cd atomic pairs and are presented in Tables 1 – 3. The tables are based on a block size of 100 atoms. The independence of the estimated and observed values in the contingency tables was evaluated by using X^2 statistics and compared with χ^2 distribution for nine degrees of freedom. The X^2 values calculated for Cd-Mg, Cu-Mg and Cu-Cd are 181.02, 6.97 and 7.23, respectively. Thus, the probabilities of random distribution, χ^2 , for the three pairs of solute atoms are 3.1×10^{-34} , 0.64 and 0.61, respectively. The extremely low value of the Cd-Mg atomic pair means that the null hypothesis that Cd and

Mg are randomly distributed is rejected. In other words, there is a strong tendency of Cd and Mg atoms to co-segregate, as seen in the atomic map.

Table 1. Contingency table for Cd and Mg in Al-Cu-Mg-Cd alloy aged at 200 °C for 15 min.

		Experimental Observations					Estimated Values					
		Mg					Mg					
		0	1	2	≥3	Total	0	1	2	≥3	Total	
Cd	0	4026	1027	168	35	5256	0	3983	1045	178	50	5256
	1	315	99	19	11	444	1	336	88	15	5	444
	2	22	14	7	6	49	2	37	10	2	0	49
	≥3	4	6	1	3	14	≥3	11	3	0	0	14
	Total	4367	1146	195	55	5763	Total	4367	1146	195	55	5763

Table 2. Contingency table for Cu and Mg in Al-Cu-Mg-Cd alloy aged at 200 °C for 15 min.

		Experimental Observations					Estimated Values					
		Mg					Mg					
		0	1	2	≥3	Total	0	1	2	≥3	Total	
Cu	0	602	164	25	0	801	0	607	159	27	8	801
	1	1103	276	45	7	1431	1	1084	285	49	13	1431
	2	1093	300	48	16	1457	2	1104	290	49	14	1457
	≥3	1569	406	77	22	2074	≥3	1572	412	70	20	2074
	Total	4367	1146	195	55	5763	Total	4367	1146	195	55	5763

Table 3. Contingency table for Cu and Cd in Al-Cu-Mg-Cd alloy aged at 200 °C for 15 min.

		Experimental Observations					Estimated Values					
		Cd					Cd					
		0	1	2	≥3	Total	0	1	2	≥3	Total	
Cu	0	746	50	4	1	801	0	730	62	7	2	801
	1	1298	117	11	5	1431	1	1305	110	13	3	1431
	2	1322	119	12	4	1457	2	1329	112	12	4	1457
	≥3	1890	158	22	4	2074	≥3	1892	160	17	5	2074
	Total	5256	444	49	14	5763	Total	5256	444	49	14	5763

Discussion

The current study confirms the earlier results [1-4, 9, 15] that the addition of minor amounts of Cd to Al-Cu alloys refines precipitation of θ' . This study also shows that the same effect occurs when minor amounts of Mg are also present. Furthermore, it has been shown that, in the quaternary Al-Cu-Mg-Cd alloy, Cd also promotes the formation of the σ phase, which is present only occasionally in the ternary Al-Cu-Mg alloy. This is a significant result given the excellent thermal stability attributed to this phase [11]. The observation of small spherical Cd particles formed throughout the matrix is consistent with considerations from the binary Al-Cd phase diagram, which indicates that Cd is immiscible in Al [10]. The small particles attached to the θ' in the aged Al-Cu-Cd alloy are confirmed to be elemental Cd. However, the small precipitates which were observed to be attached to both θ' or σ in the quaternary Al-Cu-Mg-Cd alloy were not found to be elemental Cd, but as yet unidentified Cd-Mg – rich particles. Since Cd and Mg do form intermetallic phases [10] and given the ratio of Cd and Mg found in the 3DAP experiment, it is speculated that this phase may be the MgCd compound.

Unlike the case for Sn additions to Al-Cu [4], the present observations failed to reveal any Cd or Cd-Mg – rich precipitates prior to the θ' precipitation although the 3 DAP results showed

that Cd-Mg clusters do form throughout the sample early in the ageing process. This observation supports the notion that role of clusters in assisting the nucleation is a widespread phenomenon and that the mechanism is very flexible. It is proposed that the enhancement of precipitation in this alloy is related to the prior clustering of Cd atoms in Al-Cu-Cd alloy and Cd - Mg atoms in Al-Cu-Mg-Cd alloy during the early stages of ageing. Both Cd and Mg atoms are large atoms and have high binding energies with vacancies. Therefore, these two elements may form complexes with vacancies, which produce clusters that bring together a large number of vacancies. Significantly, the clustering of these atomic species facilitates the nucleation not only of θ' , but also σ phase. Although the mechanism of nucleation is thought to be the same for the Al-Cu-(Mg, Cd) alloys studied, the mixed chemistry of the clustering in the latter case allows the co-nucleation of several Al-Cu and Al-Cu-Mg based precipitates.

Conclusions

1. In Al-4Cu-0.3Cd alloy, the θ' precipitation is enhanced and the nanoscale particles observed in the matrix and attached to θ' are confirmed to be elemental Cd.
2. The addition of Cd to the alloy Al-4Cu-0.3Mg stimulates precipitation of both θ' and the σ phase. Normally, the σ phase is observed only occasionally in the ternary alloy.
3. Co-clusters of Cd and Mg form at early stages of ageing of the Al-Cu-Mg-Cd alloy, suggesting that these clusters may initiate the enhanced precipitation and associated hardening occurring in this alloy. The mechanism in the ternary Al-Cu-Cd alloy is almost certainly the same, but the chemistry of the clusters is different.

Acknowledgements

The authors thank Prof. Barry C. Muddle, Dr. J.F. Nie and Dr. K. Raviprasad from Monash University for fruitful discussions. BTS is on leave from the Department of Metallurgy, University of Indonesia and is grateful for the provision of the Australian Development Scholarship by AusAID and the departmental scholarship by the School of Physics and Materials Engineering, Monash University.

References

1. Hardy, H.K.: J. Inst. Met., 80 (1951-52), p. 483.
2. Polmear, I.J. and H.K. Hardy: J. Inst. Met., 81 (1952-53), p. 427.
3. Silcock, J.M., T.J. Heal, and H.K. Hardy: J. Inst. Met, 84 (1955-56), p. 23.
4. Ringer, S.P., K. Hono, and T. Sakurai: Metall. Mater. Trans. A, 26A (1995), p. 2207.
5. Kanno, M., H. Suzuki, and O. Kanoh: J. Japan Inst. Light Metals, 44 (10) (1980), p. 1139.
6. Nie, J.F., B.C. Muddle, H.I. Aaronson, S.P. Ringer, and J.P. Hirth: Metall. Mater. Trans. A, in press (2002).
7. Silcock, J.M.: J. Inst. Met., 89 (1960-61), p. 203.
8. Ringer, S.P., K. Hono, I.J. Polmear, and T. Sakurai: Acta Mater., 44 (5) (1996), p. 1883.
9. Taylor, J.A., B.A. Parker, and I.J. Polmear: Met. Sci., 12 (1978), p. 478.
10. Massalski, T.B.: *Binary Alloy Phase Diagram* 2 ed. (ASM, Ohio 1990).
11. Schueller, R.D., A.K. Sachdev, and F.E. Wawner: Scripta Metall. Mater., 27 (1992), p. 617.
12. Muddle, B.C. and I.J. Polmear: Acta Metall., 37 (3) (1989), p. 777.
13. Sofyan, B.T. and S.P. Ringer: *Engineering Materials 2001*. Melbourne (2001), p.53.
14. Zhang, D.L., K. Chattopadhyay, and M. Cantor: J. Mater. Sci., 26 (1991), p. 1531.
15. Sankaran, R. and C. Laird: Mater. Sci. Eng, 14 (1974), p. 271.